The Journal of Chemical Physics

RESEARCH ARTICLE | OCTOBER 27 2026

Exceptional thermal stability of carbonic acid-rich very high-density amorphous ice

Demetrio Scelta ; Selene Berni ; Sebastiano Romi ; Samuele Fanetti ; Frederico Alabarse ; Roberto Bini

Check for updates

J. Chem. Phys. 165, 164509 (2026)
https://doi.org/10.1063/5.0347503

View Online
Export Citation

Articles You May Be Interested In

Experimental study of the polyamorphism of water. II. The isobaric transitions between HDA and VHDA at intermediate and high pressures

J. Chem. Phys. (March 2018)

Experimental study of the polyamorphism of water. I. The isobaric transitions from amorphous ices to LDA at 4 MPa

J. Chem. Phys. (March 2018)

Transitions in pressure-amorphized clathrate hydrates akin to those of amorphous ices

J. Chem. Phys. (July 2019)

28 October 2026 09:16:52

AIP Publishing

AIP Publishing
The Journal of Chemical Physics
Special Topics Open for Submissions
Learn More

The Journal of Chemical Physics ARTICLE pubs.aip.org/aip/jcp

Exceptional thermal stability of carbonic acid-rich very high-density amorphous ice

Cite as: J. Chem. Phys. 165, 164509 (2026); doi: 10.1063/5.0347503
Submitted: 10 June 2026 • Accepted: 1 October 2026 •
Published Online: 27 October 2026

View Online Export Citation CrossMark

Demetrio Scelta,[1,2,a] Selene Berni,[2,3,4] Sebastiano Romi,[2,3] Samuele Fanetti,[1,2] Frederico Alabarse,[5] and Roberto Bini[1,2,3,b]

AFFILIATIONS

[1] ICCOM-CNR, Istituto di Chimica dei Composti OrganoMetallici, Via Madonna del Piano 10, I-50019 Sesto Fiorentino, Firenze, Italy
[2] LENS, European Laboratory for Non-linear Spectroscopy, Via N. Carrara 1, I-50019 Sesto Fiorentino, Firenze, Italy
[3] Dipartimento di Chimica "Ugo Schiff," Università di Firenze, Via della Lastruccia 3, I-50019 Sesto Fiorentino, Italy
[4] IFAC-CNR, Istituto di Fisica Applicata "Nello Carrara," Via Madonna del Piano 10, I-50019 Sesto Fiorentino, Firenze, Italy
[5] Elettra Sincrotrone Trieste S.C.p.A, AREA Science Park, I-34149 Basovizza, Trieste, Italy

[a] **Author to whom correspondence should be addressed:** demetrio.scelta@cnr.it
[b] **E-mail:** roberto.bini@unifi.it

ABSTRACT

Similar to water ice, clathrate hydrates also undergo amorphization under increasing pressure at low temperature. This phenomenon was also recently reported for carbon dioxide (CO_2) clathrate hydrate and identified as a crucial step for triggering the formation of carbonic acid (H_2CO_3) molecules and their subsequent arrangement into different crystalline polymorphs upon heating. Here, we present a combined x-ray diffraction and Raman study of the amorphization of CO_2 clathrate hydrate into a high-density amorphous ice, followed by its evolution into a very-high-density amorphous (VHDA) structure. The main peculiarity of this VHDA mixed ice lies in the incorporation of a large amount of H_2CO_3 molecules, which confer exceptional stability to the amorphous phase, extending even above ambient temperature and thus largely exceeding the stability of all the amorphous ices, both pure water ice and mixed or salty ices, reported so far. Remarkably, crystallization occurs in two steps (at 4 GPa and 273 K): it first leads to the nucleation of the recently discovered metastable ice XXI, which suddenly converts to phase VII a few degrees above, allowing the nucleation of the hydrated ϵ_m-H_2CO_3 structure.

© 2026 Author(s). All article content, except where otherwise noted, is licensed under a Creative Commons Attribution (CC BY) license (https://creativecommons.org/licenses/by/4.0/). https://doi.org/10.1063/5.0347503

28 October 2026 09:16:52

INTRODUCTION

Since its discovery,[1,2] low-temperature pressure-induced amorphization (PIA) of ice Ih has been extensively investigated. Five amorphous phases have been reported: low-density (LDA), medium density (MDA), high-density (HDA), expanded high-density (eHDA), and very high-density (VHDA) (see Ref. 3 and references therein). These are distinguished by short-range structure and hydrogen bond network,[4] which reflect in different densities. These phases are relevant for explaining water anomalies,[5] as models for polyamorphism,[6,7] and because amorphous ice is abundant in the Solar System,[8,9] playing a role in geochemical and geophysical processes on icy planets and satellites. In such environments, ice is mixed with other compounds, increasing system complexity and raising interest in PIA of mixed ices, such as clathrate hydrates. As a matter of fact, at less than 140 K, clathrates transform under compression into amorphous phases similar to high-density amorphous ice.[10] This is not surprising in view of the structural analogy between the nearest neighbors arrangement of the water molecules in ice Ih and clathrate hydrates and of the low concentration of guest molecules.[11]

PIA has been experimentally observed in hydrates of Ar and Xe,[11] tetrahydrofuran (THF),[12,13] dioxolane,[14] cyclobutanone,[15] CH_4,[16,17] and C_2H_6.[17] Molecular dynamics (MD) studies provided local structural information in CH_4[18] and in THF,[13] while for CO_2 hydrates, PIA has been explored only by simulations, in relation to mechanical stability in marine sediments.[19] Simulations consistently report slow diffusion of guest molecules, avoiding phase separation

© Author(s) 2026

and preserving medium- to long-range correlations,[13,18,19] distinguishing these amorphous phases from frozen mixtures. A reduced mobility also characterizes the water network albeit the water structures of the amorphous hydrates are different from the corresponding HDA and VHDA ices.[20–22] Most of the data are gained by neutron or x-ray diffraction experiments, and spectroscopic data also confirm that cage collapse preserves the water framework, restricting guest motion while preserving short (medium) range correlation.[17]

The pressure at which PIA occurs in clathrate hydrates, in a temperature range close to 100 K, varies considerably: in THF[13] and Ar[11] hydrates around 1.3 GPa, close to pure ice; in CH_4 hydrate between 2 and 3.5 GPa;[16,17] and higher for C_2H_6[17] and Xe.[11] Differences also extend to the p–T conditions where these amorphous ices crystallize. While the stability of amorphous water ice with respect to crystallization, characterized by neutron diffraction along different p–T trajectories, never exceeds 170 K and 3 GPa,[23] amorphous methane hydrate persists to 220 K between 1.5 and 4.0 GPa,[16] where the crystallization of ice VI and ice VIII takes place, and THF to 190 K at 1 GPa.[14,15]

Annealing under pressure densifies amorphous hydrates, as shown in CH_4 hydrate by the shift of the first diffraction peak (FDP) to higher Q values[16] and confirmed by simulations (~10% density increase between 100 and 250 K at 5.5 GPa).[18] This strictly resembles the behavior of water ice, where VHDA forms.[24,25] Similarly, THF hydrate converts from HDA to VHDA upon heating under pressure.[26] Neutron scattering and molecular dynamics simulations indicate that densification arises from local water packing, with coordination increasing from 5 (HDA) to 6 (VHDA), while guest arrangements remain largely intact.

Recent studies from our group[27–29] highlighted a novel synthetic route to the formation of variously hydrated polymorphs of carbonic acid (H_2CO_3) through the low temperature compression and the subsequent isobaric heating to room temperature of pristine CO_2 clathrate hydrate.[27,28] In this experimental framework, while trying to rationalize the earlier detection of crystalline carbonic acid during diamond anvil cell (DAC) loading near liquid nitrogen temperature,[29] we observed PIA of CO_2 hydrate.[27,28] Amorphization occurred at 130 K between 1.2 and 1.5 GPa, while the formation of carbonic acid molecules, and then their organization in a hydrated ordered crystal, was detected upon increasing temperature at 4 GPa.[27–29] No such reactivity was observed in demixed CO_2-I and ice VII, underlining the role of the amorphous state obtained from the CO_2 clathrate hydrate as a reactive medium, where guest dispersion is preserved.

Here, we report an extensive characterization of this peculiar amorphous ice and its evolution upon annealing up to the formation of carbonic acid crystal, extending and complementing the findings already reported in previous studies.[27–29] Beyond acting as a crucial reactive environment, this amorphous phase is remarkable for its stability up to and above room temperature and for its complex crystallization pathway, involving the formation of the recently discovered ice metastable polymorph XXI[30,31] as an intermediate prior to the carbonic acid crystallization.

METHODS

Membrane diamond anvil cells (mDACs) equipped with IIa-type diamonds (400 μm culets) and stainless steel gaskets have been employed both for diffraction and Raman experiments. Raman spectra were measured in back scattering geometry using the 660 nm emission of a solid state diode laser. The instrumental resolution was 0.6 cm^{-1}. The synthesis of the CO_2 clathrate hydrate and both Raman and x-ray diffraction experiments were carried out using a helium closed cycle cryostat. The temperature was determined by a silicon diode placed close to the diamonds (nominal accuracy of 1 K). Pressure was measured by the shift of the ruby fluorescence wavelength[32] corrected for temperature.[33] Synchrotron angle-dispersive powder x-ray diffraction measurements were performed at ELETTRA synchrotron (XPress beamline) in transmission geometry. A PILATUS3 S 6M detector from Dectris was employed, while the x-ray beam was set to 25 KeV corresponding to a wavelength of 0.495 68 Å. The beam diameter was about 80 μm, ensuring good statistics of the sample having a ~150 μm diameter. The 2D diffraction patterns were analyzed and integrated using Dioptas software.[34]

EXPERIMENTAL RESULTS

The CO_2 clathrate hydrate was synthesized *ex situ* according to the procedure described in Refs. 27 and 28 and then transferred at liquid nitrogen temperature in the DAC. Once the sample chamber is filled with the clathrate hydrate, the DAC is closed manually and sealed by the application of pressure in membrane. During this procedure, the closing pressure cannot be easily controlled, resulting in loadings ranging from 0.5 to few GPa. Upon recovering room temperature at 3.5 GPa, the sample was mainly constituted by crystalline hydrated carbonic acid (ϵ_m phase).[27–29] The pressure was then decreased at room temperature, observing, first, the decomposition of carbonic acid into CO_2-I and ice VII, which then transforms in ice VI, followed by the melting of both species. The mixed fluid was then cooled slowly until the clathrate hydrate re-crystallization occurred, filling almost the entire sample chamber. This procedure enables the obtainment of a sample where the excess of one of the two components is severely limited. At 131 K and 0.21 GPa, the re-crystallized sI clathrate was Le Bail refined to a cell parameter a = 11.713 02 Å and then the sample was isothermally compressed. In Fig. 1, the diffraction patterns measured during this compression are shown.

Interestingly, no evidence is provided by either XRD (see Fig. 1) and Raman data (see Fig. S1 in the supplementary material) of the phase transition to the high-pressure phase reported by Hirai *et al.*[35] around 0.6–0.7 GPa. A good quality of the XRD data is maintained up to about 1 GPa, while above this pressure, the diffraction peaks of the sI phase are considerably broadened and some of them are split, an evidence of a distortion of the cubic cell. The intensity of the XRD crystalline pattern decreases as the pressure further increases, and above 1.4 GPa, only three broad and weak peaks, apparently residual of hydrate reflections, and four peaks from excess CO_2 are observable superimposed on a broad feature extending between Q values of 2 and 3 $Å^{-1}$ (see Fig. 2).

The appearance in the neutron or x-ray diffraction pattern of the broad first diffraction peak (FDP) peak, a characteristic trait of amorphous solids, is related to the presence of short-range order also providing useful information about the density (peak maximum) and the correlation length (linewidth) of the amorphous phase.[36] The behavior of our sample closely resembles what has been reported upon compression of ice Ih at 100 K,[37] thus posing some

28 October 2026 09:16:52

© Author(s) 2026

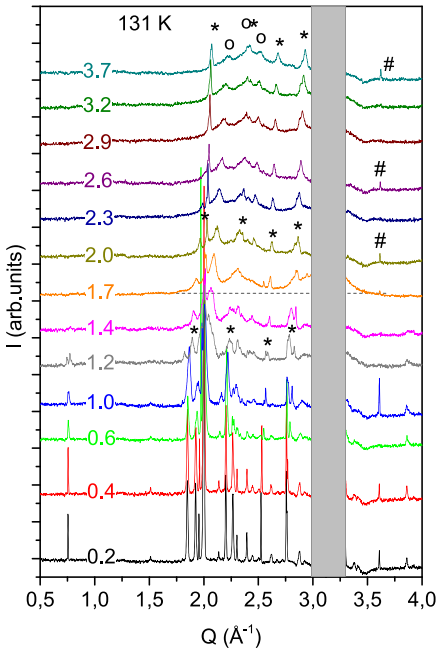

FIG. 1. Pressure evolution (values are in GPa) during the compression at 131 K of type I (sI) CO_2 clathrate hydrate. The asterisks, circles, and hash mark the CO_2-I, the clathrate hydrate remnants, and the ruby diffraction peaks, respectively. The dotted line at 1.7 GPa is a guide for the eye to highlight the appearance of the broad first diffraction peak (FDP) during amorphization of the CO_2 clathrate hydrate. Above 3 GPa, the sharp CO_2 peak at 2.4 $Å^{-1}$ is obscured by the broader central peak due to clathrate hydrate remnants.

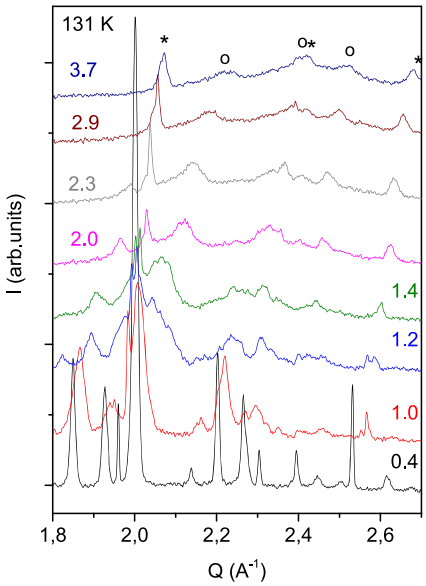

FIG. 2. Detail of the *Q* range where the first diffraction peak (FDP) of the amorphous phase appears. The asterisks indicate the CO_2-I diffraction peaks whereas the three central broad features (2.22, 2.40, and 2.52 $Å^{-}1$) visible at 1.4 GPa and persisting at higher pressures are likely remnants of the hydrate crystal phase. They are highlighted by the circles. Pressure values are expressed in GPa.

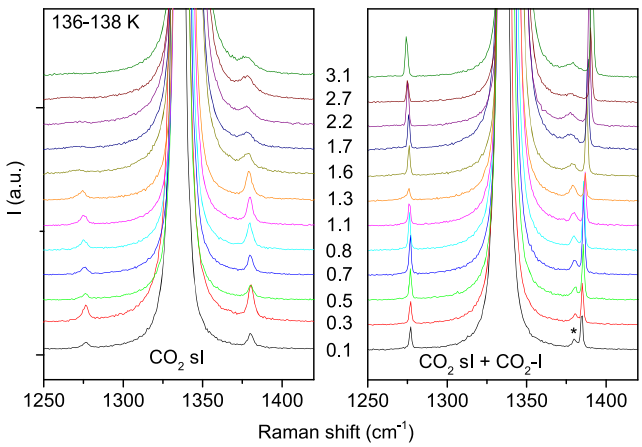

FIG. 3. Raman spectra measured in the Fermi resonance ν_1 and $2\nu_2$ region upon compression at 137(1) K. Left panel: pure sI CO_2 clatrate hydrate; right panel: simultaneous probing of pure CO_2-I and sI CO_2 clathrate hydrate. The asterisk indicates the Ω^+ Fermi component of the clathrate hydrate.

doubts about what we are effectively observing: the amorphization of CO_2 clathrate hydrate or its decomposition and the ice amorphization. This second hypothesis can be reasonably discarded on the basis of both XRD and Raman data. In the XRD patterns, the peaks relative to CO_2 were already present before the amorphization, being related to small amount of segregated CO_2 crystallites, and do not intensify when and after the sample starts to amorphize.

This is also confirmed by the Raman spectra: the regions where the peaks relative to CO_2-I are observed do not increase in number and extension. In addition, the internal modes of CO_2 encaged in the collapsed water structure are rather different from those of CO_2-I, thus confirming its capillary distribution within the amorphous phase. The spectra measured in the Fermi resonance ν_1 and $2\nu_2$ region upon compression at 137(1) K are reported in Fig. 3. The left panel of Fig. 3 shows the spectra measured in a sample region where only the sI clatrate hydrate is present, whereas in the right panel, CO_2 phase I is also probed. The comparison allows appreciating how informative is this region: the high-frequency Fermi component Ω^+ of the clathrate can be easily distinguished from that of pure CO_2-I since it is red shifted by about 5 cm^{-1} at 0.1 GPa, separation which further increases upon rising pressure. On the contrary, Ω^- is almost coincident in the clathrate hydrate and pure CO_2-I. As mentioned above, the spectrum does not change where Hirai *et al.*[35] suggest the transition to the HP phase, while a clear and sudden broadening of both Fermi components occurs at the amorphization threshold. Interestingly, the Ω^+ component, albeit broader, remains the only one clearly visible above 1.6 GPa, well distinguishable from that of CO_2-I and monotonically red shifting upon increasing pressure. This is a sharp confirmation of the preservation of the local environment and, therefore, of the widespread and ordered (short-medium range) distribution of CO_2 molecules within the amorphous ice.

The presence of a residual structure superimposed on the FDP was also reported in the structure factor [S(Q)] of the unannealed

28 October 2026 09:16:52

© Author(s) 2026

amorphous phase of both THF and CH_4 hydrates from neutron scattering experiments.[13,16] In both cases, the FDP appeared split, with maxima separated by about 0.2 $Å^{-1}$ at 3–4 GPa and 100 K, and at 1.2 GPa and 130 K for CH_4 and THF, respectively. This splitting, attributed to different length scales of the H_2O–H_2O and H_2O–guest interactions,[13,16] seems in our case more likely connected to the preservation of a residual order, as indicated by the patterns reported in Fig. 2. Upon thermal annealing, these features vanish (see Fig. 4) and the FDP peak shifts to higher Q values.[13,16] In the THF hydrate, the FDP of the annealed amorphous phase is centered at about 2.35 $Å^{-1}$ at 1.2 GPa and 130 K,[13] whereas it is at about 2.50 $Å^{-1}$ at 3.9 GPa and 220 K in the amorphized CH_4 hydrate.[16]

A consistent behavior is observed in the diffraction patterns that we measured upon increasing temperature under nearly isobaric conditions at 3.9(5) GPa and is shown in Fig. 4. As stated before, the three broad peaks residual of the clathrate structure (2.22,

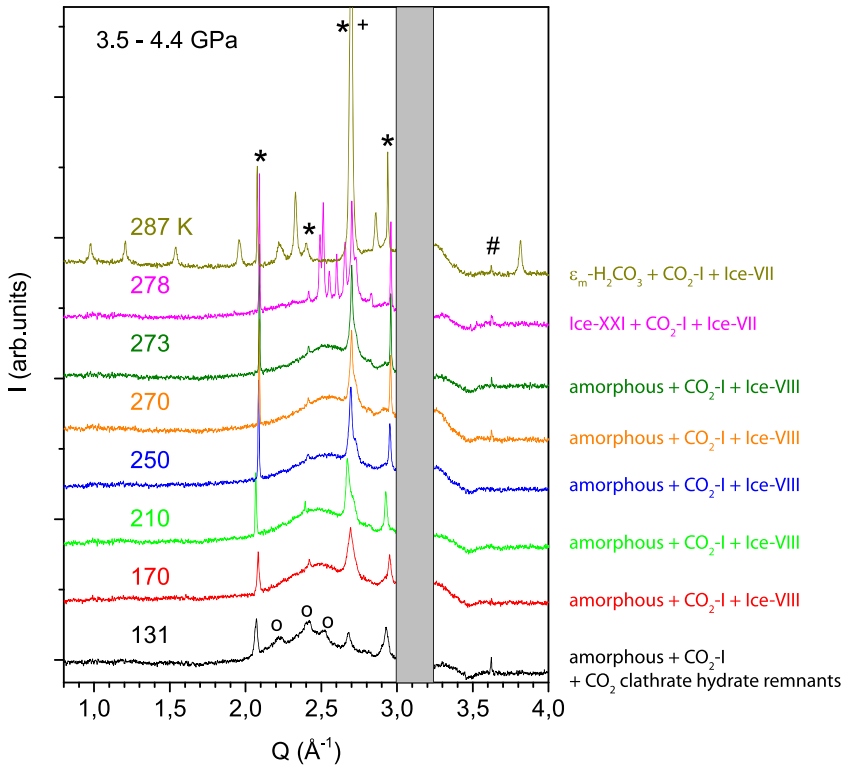

FIG. 4. Temperature evolution of the diffraction pattern of the amorphized clathrate hydrate along the quasi-isobaric thermal annealing. The asterisks and hash mark the CO_2-I and ruby diffraction peaks, respectively. The circles over the 131 K pattern locate the broad remnants from the CO_2 clathrate hydrate. The intensity of the strongest peak at 2.70 $Å^{-1}$ at 287 K is mostly due to ice VII (highlighted by a + sign). In the patterns recorded at lower temperatures, the peak asymmetry observed at this Q value is likely due to the strongest ice VIII diffraction peak. The gray region hides the strong diffraction peak from the gasket material (stainless steel).

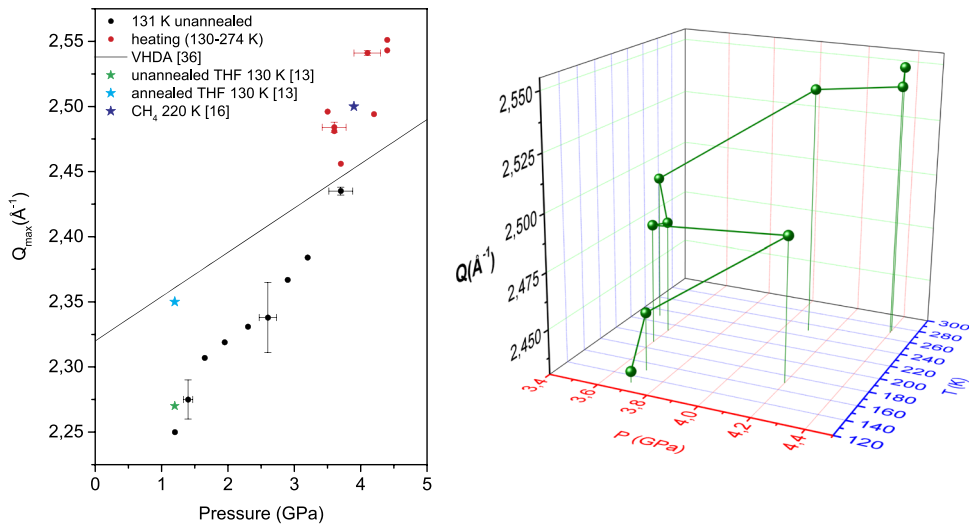

FIG. 5. Left panel: pressure evolution of the maximum of the first diffraction peak (FDP) along the compression at 131 K (black dots) and the following quasi-isobaric thermal annealing (red dots). FDP maxima from other amorphized hydrates are reported for comparison. The error in the FDP determination is larger at low pressure due to the lower intensity of the peak and to the presence of several peaks remnants of the crystalline hydrate phase. Right panel: the same data collected along the heating path are reported to highlight the effect of both pressure and temperature on the FDP peak maximum.

28 October 2026 09:16:52

© Author(s) 2026

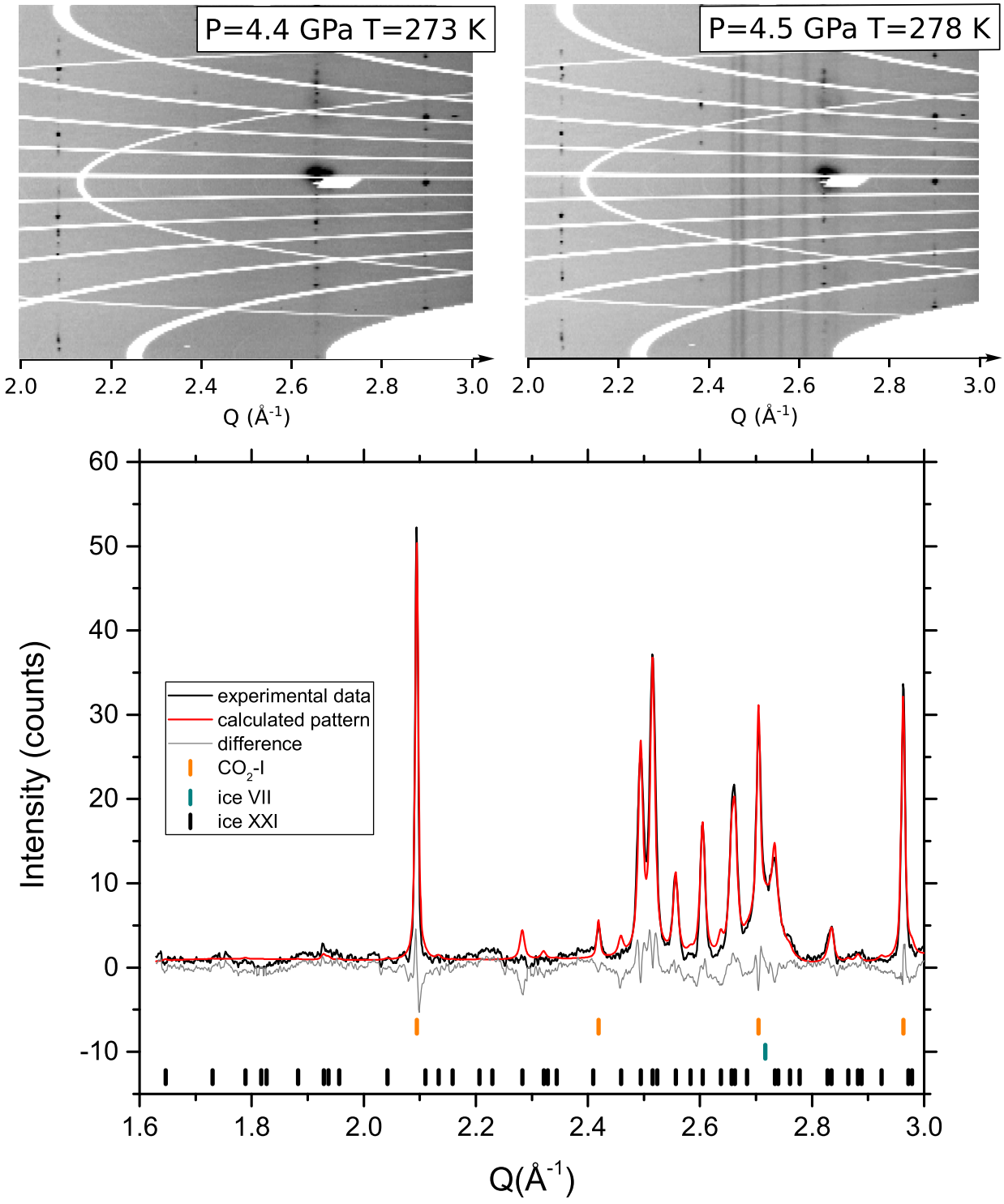

FIG. 6. Upper panel: comparison between 2D detector images acquired before (left; 273 K and 4.4 GPa) and after (right; 278 K and 4.5 GPa) crystallization to highlight the difference of the powder quality between CO_2 and the forming ice XXI. Lower panel: Rietveld refinement with the tetragonal structure $I\bar{4}2d$ of ice XXI,[30] ice VII,[40] and CO_2-I[41] of the observed pattern in the Q range between 2.0 and 3.0 $Å^{-1}$ (FDP region) at 278 K and 4.5 GPa (Rw% = 13.595%, GOF = 0.93). The obtained lattice parameters of ice XXI are $a = b = 19.4516(7)$ Å and $c = 7.5281(4)$ Å.

28 October 2026 09:16:52

© Author(s) 2026

2.40, and 2.52 $Å^{-1}$) already disappear at 170 K, and only the four diffraction peaks of CO_2-I (2.07, 2.43, 2.70, 2.95 $Å^{-1}$), and the 112 reflection of ice VIII that likely causes the asymmetry of the CO_2 reflection at 2.7 $Å^{-1}$, are still observable as imposed on the FDP of the amorphous fraction.

As already mentioned, the Q value of the peak maximum correlates with the density and its increase as a function of pressure or temperature is usually employed to follow the densification of amorphous ices. In Fig. 5, we have reported the shift of the FDP maximum along the isothermal compression and the following nearly isobaric heating. The observed monotonic increase with pressure clearly displays a progressive densification upon compression, leading, according to the available literature data,[13,16,38] to values similar to those displayed by a VHDA ice also without thermal annealing. Upon heating, the shift to larger Q values is more pronounced also in consideration of the small pressure variation. This is better appreciated on the right panel of Fig. 5, where it is highlighted how both the increase in pressure and temperature promote densification, with pressure drops compensated by temperature increases.

The temperature evolution at 4 GPa is almost the same as that of the amorphized methane hydrate that, however, is not stable above 220 K. It should be remarked that at this temperature, carbonic acid is already present in the amorphous structure, likely contributing to its stabilization.[27,28] Another parameter to be evaluated is the width of the FDP, which provides a clue of the ordering length. In our case, the fits of the FDP in the various patterns yield FWHM values scattered between 0.35 and 0.50 $Å^{-1}$ and not showing any dependence both on pressure and temperature, thus suggesting that after the collapse of the hydrate crystal structure, no macroscopic changes of the short range ordering of this amorphous mixed ice are observed.

A particularly interesting aspect, to the best of our knowledge never reported in the case of amorphous ices, is the detailed pressure evolution of the lattice modes region. Essentially, as long as we are dealing with HDA mixed ice, we observe a structure superimposed on the high-frequency side of the liquid-like tail of the Rayleigh band. However, this structure becomes perfectly defined upon the achievement of VHDA mixed ice (around 4 GPa) and remains almost unchanged up to the formation of carbonic acid molecules, when a weakening in intensity and a substantial loss of the structure are observed (see Fig. S2).

Apart from the shift at higher Q values, the diffraction pattern does not modify with increasing temperature up to 273 K (see Fig. 4). Above this temperature, crystallization occurs abruptly, with several sharp peaks appearing between 2.45 and 2.90 $Å^{-1}$, therefore, entirely enclosed in the Q range of the FDP. A further temperature increase of a few degrees determines the complete disappearance of these diffraction peaks and the appearance of the characteristic diffraction pattern of ϵ_m-H_2CO_3.[27–29] It is important to emphasize the contextual intensification of the peak at 2.7 $Å^{-1}$, assigned, at lower temperatures, to CO_2 and ice VIII. However, since all other CO_2 diffraction peaks remain essentially unchanged, the strong intensification of this peak could be ascribed to the formation of a consistent additional amount of ice VII that is the thermodynamic stable phase of water ice under these p–T conditions.

The crystallization of metastable ice phases from high density amorphous ices has been reported by several authors (see Ref. 39 and references therein). Typically, mixtures of different polymorphs are obtained with relative amounts, depending on pressure and heating rates.[39] Attempts to reproduce the peculiar diffraction pattern observed at 278 K before the carbonic acid crystallization with single ice phases, or their possible combinations, were unsuccessful until we tried the recently discovered metastable ice phase XXI, independently reported in two different studies by Lee *et al.*[30] and Kobayashi *et al.*[31] This phase was indeed found to form during the dynamic compression of supercompressed water[30] and also by heating emulsified HDA ice above 200 K at 2.5 GPa:[31] this last path, in particular, is quite similar to the p–T path we followed in our experiments. The structure of ice XXI has been resolved as body-centered tetragonal $I\bar{4}2d$ with lattice parameters at 1.6 GPa $a = b = 20.197$ Å, $c = 7.891$ Å.[30] In Fig. 6, the experimentally measured pattern is shown together with the Rietveld refinement performed using the structural data from Ref. 30, thus obtaining the lattice parameters as $a = b = 19.4516(7)$ Å and $c = 7.5281(4)$ Å. Their reduction qualitatively accounts for the different pressures, 4.5 and 1.6 GPa, of the two experiments. It is important to highlight that not only the position of the peaks but also their intensities are well reproduced. This is due to the excellent quality of the powder, as can be appreciated in the upper right panel of Fig. 5. Ice XXI was observed to be quite stable: while maintaining the pressure and temperature conditions constant, three different patterns were measured over a period of 20 min before raising the temperature again, without observing any change compared to the one shown in Fig. 6.

Contextually, the Raman spectra measured in the low frequency region along a different experimental run following the same p–T path (see Fig. S4) highlight the appearance of a peculiar lattice phonon profile. The broad and unstructured band characteristic of the amorphous phase disappears and is replaced by a spectrum of the lattice modes, featuring at least eight bands that cannot be solely attributed to the ϵ_m phase of carbonic acid or to any other known ice phase. Upon further heating to 278 K, the lattice phonon region evolves through the appearance of the expected spectrum of ϵ_m-H_2CO_3 and ice-VII.[27,29] Obviously, since there is no Raman characterization of pure ice XXI available in the current scientific literature, we cannot be sure that the spectrum recorded at 4.1 GPa and 277.5 K effectively corresponds to phase XXI; but if it does, it would clearly confirm that the crystallization of this amorphous mixed ice proceeds through this recently discovered metastable ice phase.[30,31]

DISCUSSION AND CONCLUSIONS

Amorphization of the CO_2 clathrate hydrate presents several similarities with pure ice and other clathrates hydrates. Amorphization conditions are close to those of ice Ih,[37] THF,[13] and argon hydrates.[11] In addition, decomposition is not observed, and the low frequency Raman spectra as well as the residual structure observed within the first diffraction peak (FDP) upon compression suggest the preservation of a homogeneous distribution and a short-medium range order of the CO_2 molecules, previously invoked as the key factors enabling carbonic acid formation.[27,28] Another common feature is represented by the densification of the amorphous fraction observed during compression at 130 K and subsequent isobaric heating. At amorphization, the FDP maximum matches u-HDA values[38] and unannealed amorphous THF hydrate.[13] Further compression to

28 October 2026 09:16:52

© Author(s) 2026

4 GPa yields typical VHDA ice Q values,[38] while annealing leads to even higher densification, with Q values (2.55 $Å^{-1}$ at 273 K) overcoming those reported for methane hydrate[16] and reflecting the extended stability of this amorphous phase above 273 K. Stability range and Q values better agree with those reported for salty ices where the incorporation of a certain amount of salt (LiCl, LiBr, and NaCl) expands the stability of these mixed amorphous ices close to 273 K.[42–45] The mechanism by which ions stabilize salty amorphous ices is not fully understood. Simulations indicate that ions affect the achievement of the correct orientation of water molecules required for nucleating ice VII or VIII. Heating enhances thermal motion, which both promotes ion diffusion and facilitates correct water orientations for crystallization.[42] In terms of FDP maxima, density, and p–T instability thresholds, our system closely resembles salty ices but, notably, the amorphous phase from the cold-compressed CO_2 clathrate hydrate is reportedly stable up to 6.5 GPa and 370 K.[29]

The main peculiarity of the amorphous phase obtained from the CO_2 clathrate hydrate is the formation of carbonic acid molecules at around 200 K.[27,28] The presence of these molecules may hinder ice nucleation by reducing the number of neighboring water molecules and by forming up to six H-bonds through both donors and acceptors. Such effects could, therefore, significantly increase the energetic cost of reconstructing the local environment needed for ice crystal nucleation. Important differences between the crystallization of this VHDA mixed ice and salty amorphous ices concern with the formation of ice VII and the much larger p–T stability range of carbonic acid-rich amorphous ice. In salty ices, ice VII forms progressively upon heating above 260 K,[42–44] whereas in our case, it is anticipated by the sudden appearance of ice XXI. Although the strength of hydrogen-bond interactions is lower than, or at most comparable with, that of the ion–dipole interactions that characterize salty ices, the reported differences can be ascribed to the large number of hydrogen bonds that can be formed by carbonic acid molecules.

Another interesting aspect of this process is represented by the appearance at the crystallization onset of Bragg peaks, and likely lattice phonon modes, attesting the formation of the recently discovered ice XXI.[30,31] This metastable phase is detected at 278 K and 4.5 GPa and, upon temperature increase, is replaced by the formation of ice VII and by the contextual nucleation of the ϵ_m-H_2CO_3 phase. Crystallization of amorphous ices through metastable intermediate phases is not a novelty. Considering the available data regarding both pure ice and clathrate hydrates, pressure appears as the key factor in selecting the crystallization product, which is very often composed by two or more ice phases (see Ref. 39 and references therein). For amorphized clathrate hydrates, only the crystallization of amorphous methane hydrate into ice VI or VIII, depending on the pressure, is reported.[16] Crystallization of HDA water ice upon isobaric heating (P < 2 GPa) results in different ice polymorphs (I, III, IV, V, VI, VII, IX, and XII), depending on pressure and heating rates, which very often crystallize simultaneously (see Ref. 39 and references therein). In the large majority of these studies, the diffraction analysis was performed on quenched recovered materials, whereas Klotz *et al.* monitored *in situ* the crystallization of HDA ice up to 3.9 GPa by neutron diffraction.[23] Mixtures containing ice XII and ice IV (0.7 GPa) as well as ice XII and ice VI (1.0–1.5 GPa) were detected upon nearly isobaric heating, whereas mixed ice VII/VIII formed above 3.0 GPa upon compression at 100 K. Compression of HDA ice at 77 K revealed instead the formation of ice XII.[46] Ice XII was also obtained by compressing hexagonal ice Ih above 1 GPa and temperatures lower than 150 K,[47,48] conditions analogous to the formation of the amorphous phase and thus revealing a clear competition between crystallization of ice XII and amorphization. According to the pressure conditions where we heated the sample, ice VII should crystallize from the amorphous phase. However, VHDA ice and ice VII are characterized by quite different densities,[49,50] whereas the density of ice XXI (1.417 g/cm^3 by our structure refinement at 4.5 GPa) better fits that of VHDA ice. All these features let us speculate about a possible similarity in the microscopic structure of our VHDA mixed ice and ice XXI, with the latter acting as intermediate metastable ice structure, which then converted into the thermodynamic stable ice VII. Raising the temperature to 278 K indeed leads to the formation of high-quality ϵ_m-H_2CO_3 and the contextual transformation of the metastable ice XXI into ice VII, whose diffraction peak strongly intensifies. The lattice parameter a of cubic ice VII determined from our diffraction data (a = 3.276 55 Å at 4.4 GPa and 287 K) is perfectly consistent with the values reported in the literature (a = 3.2634 Å at 4.8 GPa and 298 K,[49] and a = 3.289 22 Å at 4.2 GPa and 300 K[51]) under similar pressure and temperature conditions, making it possible to exclude the incorporation of carbonic acid molecules, or possibly residual CO_2, into ice VII, as reported instead for salty ices.[42] A thorough comparison of the volume of metastable ϵ_m-H_2CO_3 polymorph with that of the stable ϵ phase, also supported by Raman spectra, indicates two disordered water molecules per unit cell, suggesting that ϵ_m-H_2CO_3 is a kinetically trapped intermediate.[27–29] Assuming an ideal clathrate filling, the CO_2:H_2O ratio (1:6) in the starting sample becomes 1:5 H_2CO_3:H_2O after the reaction; in ϵ_m-H_2CO_3, the ratio is 1:1, implying a large water excess and substantial molecular diffusion. The formation of phase VII and the associated energy release may facilitate the concurrent ϵ_m-H_2CO_3 formation. The emergence of a hydrated structure can reasonably be attributed to the strong hydrogen bonding established in the amorphous phase among water and carbonic acid molecules.

In conclusion, the carbon dioxide clathrate hydrate undergoes low-temperature, pressure-induced amorphization under conditions nearly identical to those of ice Ih. Its pressure and temperature evolution closely resembles other amorphized clathrate hydrates. In particular, pressure increase leads to densification, with Q values of the FDP typical of those reported for VHDA ices. This process is accompanied by intensification and structuring of the lattice phonon region, not reported in previous studies. Further densification occurs during thermal annealing at 4 GPa, as revealed here by the achievement of the highest Q values reported so far in the literature among analogous systems. The exceptional stability of this VHDA mixed ice, surpassing that of salty ices and reportedly extending well above ambient temperature,[29] can be attributed to the presence of carbonic acid molecules which form during thermal annealing, as revealed by Raman spectroscopy (see Fig. S3).[27,28] The uniform distribution within the amorphous phase originates a complex hydrogen-bonded network involving both water and H_2CO_3 molecules, which inhibits or slows down the diffusion of water molecules toward nucleation sites, thereby affecting the crystallization of water ice polymorphs. Remarkably, between the VHDA mixed ice and the carbonic acid crystalline polymorph forming above 278 K, a transient phase is detected at 278 K, identified as the

28 October 2026 09:16:52

© Author(s) 2026

recently discovered metastable ice XXI. This polymorph, first discovered during dynamic compression of supercompressed water as a precursor to ice VI crystallization under milder pressure conditions, exhibits a noteworthy temporal stability that, from our experiments, extends at least for tens of minutes.

This study has implications from a geophysical perspective. As far as CO_2 is concerned, the amorphous phase provides an additional solid form, along with clathrate hydrates or filled ices, for sequestering carbon materials in the icy mantles of water-rich systems. The occurrence of high-pressure ice polymorphs in the interiors of planets and icy satellites is well established, playing a key role in determining their physical properties. Our findings, revealing the persistence of mixed amorphous ices in a wide p–T range, congruent for example with the Titan geotherm,[52] highlight the potential importance that amorphous ices containing a consistent amount of H-bonded molecules may have in shaping the characteristics of the icy material present in the depth and then the behavior and evolution of such celestial bodies. Beyond their relevance to planetary science, amorphous ices provide a unique molecular environment in which the hydrogen-bonded water network and trapped guest molecules can give rise to structural, reactive, and kinetic behaviors that differ fundamentally from that of crystalline ice. From a chemical and physical perspective, these systems offer a valuable platform for probing how hydrogen-bond topology, local molecular environments, and guest–host interactions regulate molecular mobility, reactivity, and phase stability in a highly disordered, non-equilibrium solid. In particular, the reactivity and remarkable stability of guest-containing amorphous ices raise broader questions concerning the coupling between molecular diffusion and chemical transformation, the microscopic mechanisms governing crystallization, and the role of trapped species in modifying the free-energy landscape of metastable solids. These questions are relevant not only to ice chemistry but also to fundamental problems in physical chemistry and condensed-matter physics, including hydrogen-bond network dynamics, molecular transport in disordered media, glass-like relaxation, and nucleation and phase-transition kinetics. We, therefore, believe that our findings provide insights into the general principles governing the structure, reactivity, and stability of metastable molecular solids, with relevance well beyond their specific planetary implications.

SUPPLEMENTARY MATERIAL

See the supplementary material for additional Raman data about low temperature compression and isobaric heating of the sample as well as for the characterization of the lattice phonon bands of the intermediate metastable ice phase.

ACKNOWLEDGMENTS

The authors acknowledge the funding provided by project IPHOQS, CUP: B53C22001750006. The authors also acknowledge the financial support obtained under the National Recovery and Resilience Plan (NRRP), Mission 4, Component 2, Investment 1.1, Call for tender No. 104 published on 2/2/2022 by the Italian Ministry of University and Research (MUR), funded by the European Union-NextGenerationEU, Project Title: Pressure induced photoreduction of CO_2 inside inorganic and metal organic porous materials, CUP B53D23025660001, Grant Assignment Decree No. 1384 adopted on 01/09/2023 by the Italian Ministry of Ministry of University and Research (MUR). This research was also funded by the European Union- NextGeneration EU, within PRIN 2022, PNRR M4C2, Project E-ICES, Project Title: Probing the Exotic properties of gas and ions filled ICES under extreme conditions: from planetary interiors modeling to hydrogen storage and green Energy applications 2022NRBLPT and CUP B53D23004390006. The authors acknowledge the Elettra Sincrotrone Trieste for the provision of synchrotron radiation facilities (Proposal No. 20245138) and thank F. Alabarse for his assistance in using beamline XPress. S.B. acknowledges the CNR-FOELENS project.

AUTHOR DECLARATIONS

Conflict of Interest

The authors have no conflicts to disclose.

Author Contributions

Demetrio Scelta: Conceptualization (equal); Data curation (equal); Formal analysis (equal); Investigation (equal); Methodology (equal); Writing – original draft (equal); Writing – review & editing (equal). **Selene Berni**: Conceptualization (equal); Data curation (equal); Formal analysis (equal); Investigation (equal); Methodology (equal); Writing – review & editing (equal). **Sebastiano Romi**: Conceptualization (equal); Data curation (equal); Formal analysis (equal); Investigation (equal); Methodology (equal); Writing – review & editing (equal). **Samuele Fanetti**: Conceptualization (equal); Data curation (equal); Formal analysis (equal); Investigation (equal); Methodology (equal); Writing – review & editing (equal). **Frederico Alabarse**: Methodology (equal); Writing – review & editing (equal). **Roberto Bini**: Conceptualization (equal); Data curation (equal); Formal analysis (equal); Funding acquisition (equal); Investigation (equal); Methodology (equal); Supervision (equal); Writing – original draft (equal); Writing – review & editing (equal).

DATA AVAILABILITY

The data that support the findings of this study are available from the corresponding author upon reasonable request.

REFERENCES

[1] O. Mishima, L. D. Calvert, and E. Whalley, "'Melting ice' I at 77 K and 10 kbar: A new method of making amorphous solids," Nature **310**, 393–395 (1984).

[2] O. Mishima, L. D. Calvert, and E. Whalley, "An apparently first-order transition between two amorphous phases of ice induced by pressure," Nature **314**, 76–78 (1985).

[3] A. Rosu-Finsen, M. B. Davies, A. Amon, H. Wu, A. Sella, A. Michaelides, and C. G. Salzmann, "Medium-density amorphous ice," Science **379**, 474–478 (2023).

[4] F. Martelli, N. Giovambattista, S. Torquato, and R. Car, "Searching for crystal-ice domains in amorphous ices," Phys. Rev. Mater. **2**, 075601 (2018).

28 October 2026 09:16:52

© Author(s) 2026

[5]K. Amann-Winkel, R. Böhmer, F. Fujara, C. Gainaru, B. Geil, and T. Loerting, "Colloquium: Water's controversial glass transitions," Rev. Mod. Phys. **88**, 011002 (2016).
[6]R. J. Hemley, A. P. Jephcoat, H. K. Mao, L. C. Ming, and M. H. Manghnani, "Pressure-induced amorphization of crystalline silica," Nature **334**, 52–54 (1988).
[7]M. B. Kruger and R. Jeanloz, "Memory glass: An amorphous material formed from $AlPO_4$," Science **249**, 647–649 (1990).
[8]R. Smoluchowski, "Solar system ice: Amorphous or crystalline?," Science **222**, 161–163 (1983).
[9]P. Jenniskens, D. F. Blake, and A. Kouchi, "Amorphous water ice," in *Solar System Ices*, *Astrophysics and Space Science Library*, edited by B. Schmitt, C. De Bergh, and M. Festou (Springer, Dordrecht, 1998), Vol. 227.
[10]O. Mishima, "Relationship between melting and amorphization of ice," Nature **384**, 546–549 (1996).
[11]P. H. B. Brant Carvalho, A. Mace, O. Andersson, C. A. Tulk, J. Molaison, A. P. Lyubartsev, I. M. Nangoi, A. A. Leitão, and U. Häussermann, "Pressure-induced amorphization of noble gas clathrate hydrates," Phys. Rev. B **103**, 064205 (2021).
[12]Y. Suzuki, "Evidence of pressure-induced amorphization of tetrahydrofuran clathrate hydrate," Phys. Rev. B **70**, 172108 (2004).
[13]P. H. B. Brant Carvalho, A. Mace, C. L. Bull, N. P. Funnell, C. A. Tulk, O. Andersson, and U. Häussermann, "Elucidation of the pressure induced amorphization of tetrahydrofuran clathrate hydrate," J. Chem. Phys. **150**, 204506 (2019).
[14]O. Andersson and Y. Nakazawa, "Transitions in pressure collapsed clathrates hydrates," J. Phys. Chem. B **119**, 3846–3853 (2015).
[15]O. Andersson and A. Inaba, "Glass transitions in pressure-collapsed ice clathrates and implications for cold water," J. Phys. Chem. Lett. **3**, 1951–1955 (2012).
[16]C. A. Tulk, D. D. Klug, J. J. Molaison, A. M. dos Santos, and N. Pradhan, "Structure and stability of an amorphous water–methane mixture produced by cold compression of methane hydrate," Phys. Rev. B **86**, 054110 (2012).
[17]N. Noguchi, Y. Shiraishi, M. Kageyama, Y. Yokoi, S. Kurohama, N. Okada, and H. Okamura, "Direct observation of pressure-induced amorphization of methane/ethane hydrates using Raman and infrared spectroscopy," Phys. Chem. Chem. Phys. **25**, 22161–22170 (2023).
[18]N. J. English and J. S. Tse, "Pressure-induced amorphization of methane hydrate," Phys. Rev. B **86**, 104109 (2012).
[19]P. Cao, J. Wu, and F. Ning, "Mechanical properties of amorphous CO_2 hydrates: Insights from molecular simulations," Phys. Chem. Chem. Phys. **26**, 9388–9398 (2024).
[20]D. T. Bowron, J. L. Finney, A. Hallbrucker, I. Kohl, T. Loerting, E. Mayer, and A. K. Soper, "The local and intermediate range structures of the five amorphous ices at and ambient pressure: A Faber-Ziman and Bhatia-Thornton analysis," J. Chem. Phys. **125**, 194502 (2006).
[21]J. L. Finney, A. Hallbrucker, I. Kohl, A. K. Soper, and D. T. Bowron, "Structures of high and low density amorphous ice by Neutron diffraction," Phys. Rev. Lett. **88**, 225503 (2002).
[22]J. L. Finney, D. T. Bowron, A. K. Soper, T. Loerting, E. Mayer, and A. Hallbrucker, "Structure of a new dense amorphous ice," Phys. Rev. Lett. **89**, 205503 (2002).
[23]S. Klotz, G. Hamel, J. S. Loveday, R. J. Nelmes, and M. Guthrie, "Recrystallisation of HDA ice under pressure by in-situ neutron diffraction to 3.9 GPa," Z. Kristallogr.-Cryst. Mater. **218**, 117–122 (2003).
[24]T. Loerting, C. Salzmann, I. Kohl, E. Mayer, and A. Hallbrucker, "A second distinct structural 'state' of high-density amorphous ice at 77 K and 1 bar," Phys. Chem. Chem. Phys. **3**, 5355–5357 (2001).
[25]T. Loerting, C. G. Salzmann, K. Winkel, and E. Mayer, "The relation between high-density and very-high-density amorphous ice," Phys. Chem. Chem. Phys. **8**, 2810–2818 (2006).
[26]P. H. B. Brant Carvalho, M. Ivanov, O. Andersson, T. Loerting, M. Bauer, C. A. Tulk, B. Haberl, L. L. Daemen, J. J. Molaison, K. Amann-Winkel, A. P. Lyubartsev *et al.*, "Neutron scattering study of polyamorphic THF·17(H_2O)—Toward a generalized picture of amorphous states and structures derived from clathrate hydrates," Phys. Chem. Chem. Phys. **25**, 14981–14991 (2023).
[27]S. Berni, D. Scelta, S. Romi, S. Fanetti, F. Alabarse, B. Wehinger, and R. Bini, "Understanding the formation mechanism of crystalline hydrated polymorphs of carbonic acid from CO_2 clathrate hydrate," Chem. Sci. **16**, 22769–22780 (2025).
[28]S. Berni, D. Scelta, S. Romi, S. Fanetti, F. Alabarse, B. Wehinger, and R. Bini, "Correction: Understanding the formation mechanism of crystalline hydrated polymorphs of carbonic acid from CO_2 clathrate hydrate," Chem. Sci. **17**, 1894 (2026).
[29]S. Berni, D. Scelta, S. Romi, S. Fanetti, F. Alabarse, M. Pagliai, and R. Bini, "Exploring high-pressure polymorphism in carbonic acid through direct synthesis from carbon dioxide clathrate," Angew. Chem., Int. Ed. **63**, e202403953 (2024).
[30]Y.-H. Lee, J. K. Kim, Y. J. Kim *et al.*, "Multiple freezing–melting pathways of high-density ice through ice XXI phase at room temperature," Nat. Mater. **25**, 302–309 (2026).
[31]H. Kobayashi, K. Komatsu, K. Mochizuki, H. Ito, K. Momma, S. Machida, T. Hattori, K. Hirata, Y. Kawano, S. Maki-Yonekura, K. Takaba, K. Yonekura, Q. Xue, M. Sato, and H. Kagi, "New metastable ice phases via supercooled water," arXiv:2507.14415 (2025).
[32]H. K. Mao, P. M. Bell, J. W. Shaner, and D. J. Steinberg, "Specific volume measurements of Cu, Pd, and Ag and calibration of the ruby R_1 fluorescence pressure gauge from 0.06 to 1 Mbar," J. Appl. Phys. **49**, 3276–3283 (1978).
[33]D. D. Ragan, R. Gustavsen, and D. Schiferl, "Calibration of the ruby R_1 and R_2 fluorescence shifts as a function of temperature from 0 to 600 K," J. Appl. Phys. **72**, 5539–5544 (1992).
[34]C. Prescher and V. B. Prakapenka, "DIOPTAS: A program for reduction of two-dimensional X-ray diffraction data and data exploration," High Pressure Res. **35**, 223–230 (2015).
[35]H. Hirai, K. Komatsu, M. Honda, T. Kawamura, Y. Yamamoto, and T. Yagi, "Phase changes of CO_2 hydrate under high pressure and low temperature," J. Chem. Phys. **133**, 124511 (2010).
[36]J. N. Stern and T. Loerting, "On the crystallisation temperature of very high-density amorphous ice," Phys. Chem. Chem. Phys. **20**, 12589–12598 (2018).
[37]C. Lin, X. Yong, J. S. Tse, J. S. Smith, S. V. Sinogeikin, C. Kenney-Benson, and G. Shen, "Kinetically controlled two-step amorphization and amorphous-amorphous transition in ice," Phys. Rev. Lett. **119**, 135701 (2017).
[38]R. J. Nelmes, J. S. Loveday, T. Strässle, C. L. Bull, M. Guthrie, G. Hamel, and S. Klotz, "Annealed high-density amorphous ice under pressure," Nat. Phys. **2**, 414–418 (2006).
[39]C. M. Tonauer, L.-R. Fidler, J. Giebelmann, K. Yamashita, and T. Loerting, "Nucleation and growth of crystalline ices from amorphous ices," J. Chem. Phys. **158**, 141001 (2023).
[40]B. Kamb and B. L. Davis, "Ice VII, the densest form of ice," Proc. Natl. Acad. Sci. U. S. A. **52**, 1433–1439 (1964).
[41]R. T. Downs and M. S. Somayazulu, "Carbon dioxide at 1.0 GPa," Acta Crystallogr., Sect. C: Cryst. Struct. Commun. **54**, 897–898 (1998).
[42]S. Klotz, L. E. Bove, T. Strässle, T. C. Hansen, and A. M. Saitta, "The preparation and structure of salty ice VII under pressure," Nat. Mater. **8**, 405–409 (2009).
[43]S. Klotz, K. Komatsu, F. Pietrucci, H. Kagi, A.-A. Ludl, S. Machida, T. Hattori, A. Sano-Furukawa, and L. E. Bove, "Ice VII from aqueous salt solutions: From a glass to a crystal with broken H-bonds," Sci. Rep. **6**, 32040 (2016).
[44]A.-A. Ludl, L. E. Bove, D. Corradini, A. M. Saitta, M. Salanne, C. L. Bull, and S. Klotz, "Probing ice VII crystallization from amorphous NaCl–D_2O

28 October 2026 09:16:52

© Author(s) 2026

solutions at gigapascal pressures," Phys. Chem. Chem. Phys. **19**, 1875–1883 (2017).
[45]K. Komatsu, A. Shinozaki, S. Machida, T. Matsubayashi, M. Watanabe, H. Kagi, A. Sano-Furukawa, and T. Hattori, "Crystal structure of magnesium dichloride decahydrate determined by X-ray and neutron diffraction under high pressure," Acta Crystallogr., Sect. B: Struct. Sci., Cryst. Eng. Mater. **71**, 74–80 (2015).
[46]I. Kohl, E. Mayer, and A. Hallbrucker, "Ice XII forms on compression of hexagonal ice at 77 K via high-density amorphous water," Phys. Chem. Chem. Phys. **3**, 602–605 (2001).
[47]M. Koza, H. Schober, A. Tölle, F. Fujara, and T. Hansen, "Formation of ice XII at different conditions," Nature **397**, 660–661 (1999).
[48]M. M. Koza, H. Schober, T. Hansen, A. Tölle, and F. Fujara, "Ice XII in its second regime of metastability," Phys. Rev. Lett. **84**, 4112–4115 (2000).
[49]S. Klotz, K. Komatsu, H. Kagi, K. Kunc, A. Sano-Furukawa, S. Machida, and T. Hattori, "Bulk moduli and equations of state of ice VII and ice VIII," Phys. Rev. B **95**, 174111 (2017).
[50]J. K. Christie, M. Guthrie, C. A. Tulk, C. J. Benmore, D. D. Klug, S. N. Taraskin, and S. R. Elliott, "Modeling the atomic structure of very high-density amorphous ice," Phys. Rev. B **72**, 012201 (2005).
[51]L. Bezacier, B. Journaux, J.-P. Perrillat, H. Cardon, M. Hanfland, and I. Daniel, "Equations of state of ice VI and ice VII at high pressure and high temperature," J. Chem. Phys. **141**, 104505 (2014).
[52]F. Sohl, A. Solomonidou, F. W. Wagner, A. Coustenis, H. Hussmann, and D. Schulze-Makuch, "Structural and tidal models of Titan and inferences on cryovolcanism," J. Geophys. Res. Planets **119**, 1013–1036, https://doi.org/10.1002/2013je004512 (2014).

28 October 2026 09:16:52

© Author(s) 2026